

# 4

## ***Cyclohexanone role during the synthesis of 3-APTMS mediated AuNPs and its comparison with other mild reducing agents***

---

---

### **4.1. INTRODUCTION**

The requirements for practical usability of gold nanoparticles in a variety of organic and aqueous solvent have directed the use of bipolar organic reagents in the synthesis of functional nanoparticles. The use of 3-APTMS has been very well documented as a potential stabilizer for noble metal nanoparticles (Saha et al., 2012). Detailed investigation on the role of 3-APTMS during the synthesis of noble metal nanoparticles that required the participation of 3-APTMS compatible organic reducing agents, like 3-glycidoxypropyltrimethoxysilane (3-GPTMS) (Pandey and Chauhan.,2012)and tetrahydrofuranhydroperoxide (THF-HPO) has been discussed in previous chapters. During the course of AuNPs synthesis, these reducing agents interact in different methods with 3-APTMS, resulting in the formation of organic moiety dependent reaction products that may alter the inherent properties of as synthesized AuNPs. Such products may also influence the dispersion ability of the resulting AuNPs in different polar and non-polar

solvents for specific application, due to the bipolar nature of 3-APTMS and the polarity/non-polarity of the organic reducing agents. The AuNPs made using 3-APTMS and 3-GPTMS in methanol are mostly dispersible in organic solvents as discussed in chapter two. Similarly, the use of THF–HPO with 3-APTMS (chapter three) during such synthesis resulted in AuNPs dispersible largely in aqueous medium. The dependence of the reducing agent on the solvent required for the synthesis of AuNPs resulted in differential kinetic limitation when allowed to interact with 3-APTMS capped Au<sup>3+</sup> ions.

The findings on the use of 3-APTMS and cyclohexanone for the synthesis of Prussian blue nanoparticles revealed that 3-APTMS capped hexacyanoferrate ions undergo controlled conversion into polycrystalline Prussian Blue (PB) with excellent electrochemical behavior for practical applications (Pandey and Pandey, 2013c). Similar processes also enable the synthesis of polycrystalline mixed metal hexacyanoferrate with nearly all combinations of transition metal ions (Pandey and Pandey, 2013a). Cyclohexanone in aqueous media shows a biphasic system, and even in such conditions the controlled synthesis of nanoparticles are recorded. Cyclohexanone (biphasic) mediated synthesis of AuNPs has been reported by Uppal et al. (2013) but the biphasic system of nanoparticles resulted in transition in nanogeometry of AuNPs with time, suggesting the need for a stabilizer. The reducing and stabilizing property of 3-APTMS with some other mild reducing agent (Pandey and Chauhan, 2012) directed the detailed examination on the role of cyclohexanone and 3-APTMS during nanoparticle conversion. Further, the use of cyclohexanone with 3-APTMS might prove effective in enhancing catalytic activity through the formation of an organic–inorganic hybrid because the interaction of functional alkoxy silane and small organic molecules result in the formation of such catalytic material (Wight and Davis, 2002). The

hydrophobic behavior of cyclohexanone and micellar activity of 3-APTMS may allow the synthesis of functional AuNPs, suitable for the formation of nanocomposites with a variety of known catalytic materials (e.g. metal hexacyanoferrate, ruthenium bipyridyl), dispersible in suitable solvents for practical bioanalytical application. Accordingly, a detailed investigation on the role of 3-APTMS mediated conversion of gold cations in the presence of cyclohexanone is sought from the following angles: (1) conversion of 3-APTMS capped gold ions to respective nanoparticles in the presence of cyclohexanone, (2) checking the dispersibility of as synthesized cyclohexanone mediated AuNPs at different ratios of 3-APTMS and cyclohexanone, (3) the ability of AuNPs to form nanocomposites displaying peroxidase mimetic ability for probing glucose oxidase catalyzed reactions. Further, the rate of 3-APTMS mediated synthesis of AuNPs may be the function of organic reducing agents and accordingly, comparisons of the roles of 3-GPTMS, THF-HPO and cyclohexanone on the following points are also undertaken: (a) time required during nanoparticles conversion as a function of organic moieties, (b) catalytic ability of nanoparticles based on functional ability and nanogeometry, (c) stability of as synthesized nanoparticles for practical applications, and (d) dispersibility of as synthesized nanoparticles in different solvents as a function of organic moieties. The results on these lines are reported in this chapter.

## **4.2. EXPERIMENTAL**

### **4.2.1. Materials and methods**

3-Aminopropyltrimethoxysilane, 3-GPTMS, chloroauric acid and o-dianisidine were obtained from Aldrich Chem. Co.; cyclohexanone was obtained from S.D. Fine-Chem. Pvt.

Ltd.; toluene, hydrogen peroxide, ethyl acetate, dichloromethane and acetonitrile were obtained from Merck, India. All other chemicals employed were of analytical grade. Aqueous solutions were prepared by using double distilled-deionized water (Elga water purification system). All the experiments were performed at room temperature unless otherwise mentioned. The absorption spectra of nanoparticles were recorded using a Hitachi U-2900 Spectrophotometer. Transmission electron microscopy (TEM) studies were performed using Morgagni 268D (Fei Electron Optics) and electrochemical measurements were made with electrochemical workstation CHI 660B (CHI instrument, USA).

#### **4.2.2. 3-APTMS and cyclohexanone mediated synthesis of AuNPs and its nanocomposite**

In a typical procedure 1 ml sol of AuNPs was prepared by adding 100 $\mu$ l of desired concentration of 3-APTMS to 100 $\mu$ l of 0.025 M HAuCl<sub>4</sub>. The mixture was stirred using a cyclomixer for 2 min followed by the addition of 500 $\mu$ l of cyclohexanone and stirred again on the vortex mixer. Methanol was added to make up the desired volume. The reaction mixture was then left undisturbed in the dark for 1–3 h. The appearance of red, purple or blue colour of the resulting sol indicated the formation of AuNPs. The nanocomposite of PBNPs–AuNPs was made by mixing as synthesized AuNPs and Prussian blue nanoparticles (PBNPs) prepared using the same reagent 3-APTMS and cyclohexanone (Pandey and Pandey, 2013c). AuNPs (100 $\mu$ l) and PBNPs (50 $\mu$ l) were mixed by stirring and incubated for 5 minutes resulting in the formation of a homogeneous PBNPS–AuNPs sol. An aqueous solution of ruthenium bipyridyl Ru(bpy) (5 mM, 5 $\mu$ l) was added to 15 $\mu$ l of PBNPs–AuNPs sol to obtain a homogeneous dispersion of PB–AuNPs–Ru(bpy) nanocomposite.

### **4.2.3. Electrochemical measurements**

AuNPs of two sizes AuNP1 (blue) and AuNP2 (red) were sonicated with a Prussian blue Nanoparticles (PBNPs) suspension, which was made by controlled mixing of ferrous sulphate and potassium ferricyanide following a standard process. The PBNPs–AuNPs suspension was allowed to be adsorbed thoroughly on graphite particles (1–2mm) and dried at 90°C overnight. The adsorbed nanocomposite on graphite particles was incorporated within a graphite paste electrode having composition as follows: PBNPs–AuNPs 2.5% (w/w), graphite powder 67.5% (w/w), Nujol oil 30% (w/w). The well of the electrode body (MF-2010 obtained from Bioanalytical Systems, West Lafayette, IN, USA) was filled with active graphite paste. The paste surface was manually smoothed on a clean paper. Electrochemical measurements were performed in a three-electrode configuration equipped with the graphite paste electrode as the working electrode, Ag/AgCl reference and a platinum plate counter electrode with a working volume of 3 ml. All electrochemical experiments were performed in 0.1 M phosphate buffer solution (pH 7.0) containing 0.5 M KCl.

### **4.2.4. Peroxidase-like catalytic activity**

The peroxidase like activity of as synthesized nanoparticles was determined spectrophotometrically by measuring the formation of oxidized product of o-dianisidine at 430 nm ( $11.3 \text{ mM}^{-1}\text{cm}^{-1}$ ) using a Hitachi U-2900 spectrophotometer. Typically, the o-dianisidine (20 mM, 10 $\mu$ l) oxidation activity was measured in water (2 ml) in the presence of Hydrogen peroxide (10 $\mu$ l). AuNPs (5 $\mu$ l) were added to start the reaction. Glucose detection was performed as follows: (a) 40 $\mu$ l of 10 mg ml<sup>-1</sup> Glucose Oxidase and 200 $\mu$ l of

glucose at different concentrations in 0.1 M phosphate buffer (pH 7.0) were incubated at 35°C for 45 min; (b) 50µl of o-dianisidine (0.5mM), 15 µl of the PBNPs–AuNPs–Ru (bpy) and 1695µl of 0.1 M phosphate buffer (pH 7.0) were added to the above reaction solution; (c) the reaction mixture was incubated at 45°C for 30 min followed by measurement of absorption at 430 nm.

### **4.3. RESULTS**

#### **4.3.1. Requirements of organic reducing agents during 3-APTMS mediated synthesis of AuNPs**

The synthesis of AuNPs either in aqueous or organic systems have their own limitations specifically for the transfer of newly formed nanoparticles from a polar to a non-polar environment or vice versa. Such requirements may involve the use of some phase transfer reagents like ionic liquid (Wang et al., 1998; Lala et al., 2001). These limitations can be eliminated by the use of suitable reagents having bipolar behavior, together acting as both reducing and stabilizing agents during the conversion of noble metal salts into respective nanoparticles. The organic amines have shown their potential as reagents and stabilizers for the nanomaterial synthesis (Saha et al., 2012; Manikas et al., 2013; Guidelli et al., 2012). 3-APTMS acts as a potential reagent for the conversion of noble metal cations into respective nanoparticles but require the participation of additional organic reagents during nanoparticle synthesis as has been described in previous chapters. Accordingly, the role of 3-GPTMS and THF–HPO for real time synthesis of AuNPs from 3-APTMS capped Au<sup>3+</sup> has been demonstrated (Pandey and Chauhan, 2012). 3-APTMS alone does not enable the synthesis of AuNPs under similar conditions even after 24 h. The findings along these lines

have shown the organic moieties (3-GPTMS and THF-HPO) dependent behavior of the AuNPs with significant variation in their catalytic ability despite the use of 3-APTMS as one of the reagents in both cases. This difference in catalytic behavior of AuNPs as a function of 3-GPTMS or THF-HPO is due to the formation of an organic-inorganic hybrid in the later case that enhances the catalytic ability of the AuNPs. The major differences in both synthetic protocol and catalytic behavior are as follows: (1) 3-GPTMS allows the synthesis of AuNPs only in methanolic medium, whereas the same with THF-HPO takes place in water, (2) The nanoparticles made through 3-APTMS and 3-GPTMS are mostly dispersible in organic solvent with limited dispersibility in water under specific ratio of 3-APTMS/3-GPTMS, while THF-HPO and 3-APTMS mediated synthesis result in nanoparticles that are mostly dispersible in relatively more polar solvents(water) and not dispersible in organic solvents. The limited dispersibility of 3-GPTMS and THF-HPO mediated AuNPs led to the search for another reducing agent with dispersibility in a variety of solvents. Uppal et al. (2013) have observed the synthesis of AuNPs only in the presence of cyclohexanone, which is a biphasic system with transition in nanogeometry as a function of time. Accordingly, attempts on the synthesis of AuNPs utilizing cyclohexanone and 3-APTMS in a monophasic system have been performed. These findings revealed the significant role of organic reagents during 3-APTMS mediated conversion of noble metal nanoparticles and required a comparative investigation. Fig. 4.1A shows the real time synthesis of AuNPs mediated by 3-APTMS and THF-HPO, whereas Fig. 4.1B shows the similar result replacing THF-HPO with cyclohexanone. The results, as shown in Fig.4.1, clearly demonstrate the formation of AuNPs with significant variation in the use of 3-APTMS concentration when the reducing agents are changed. Cyclohexanone requires low concentration of 3-APTMS under similar conditions. It is to be noted that the synthesis of

AuNPs require methanolic medium when cyclohexanone is used as reducing agent, whereas THF– HPO enables the synthesis in water.

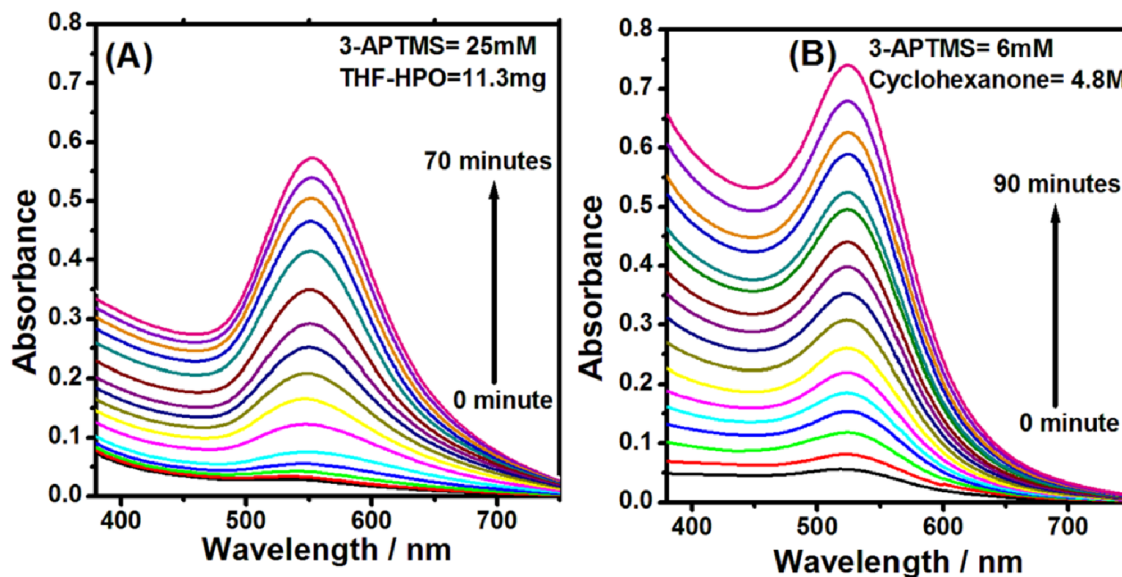


Figure 4.1. Real time synthesis of AuNPs mediated by 3-APTMS–THF–HPO (A) and 3-APTMS–cyclohexanone (B).

---

#### 4.3.2. Cyclohexanone and 3-APTMS mediated synthesis of AuNPs

Cyclohexanone enables the synthesis of AuNPs in the presence of 3-APTMS in methanolic medium under specific ratios of 3-APTMS/cyclohexanone within 0.5–3 h at room temperature. The concentrations of both the reagents significantly control the synthesis of AuNPs. The synthesis of AuNPs was investigated under two different conditions: (a) varying the concentrations of 3-APTMS while keeping the concentration of cyclohexanone constant, (b) keeping 3-APTMS concentration constant while changing the concentrations of cyclohexanone. Fig. 4.2 depicts the photograph and respective absorption maxima of AuNPs synthesized at different concentrations of 3-APTMS (3–12 mM), while keeping the concentration of cyclohexanone constant (4.8 M), displaying gradual variations

in SPR and showing the significance of 3-APTMS during AuNPs synthesis. The effect of cyclohexanone concentration on the size of AuNPs is observed under two different concentrations of 3-APTMS (5 mM and 10 mM). The higher concentration of 3-APTMS (10 mM) resulted in blue nanoparticles, whereas lower concentration (5 mM) largely gave red nanoparticles as shown in Fig. 4.3A and 4.3B, respectively. The morphology and size of as synthesized AuNPs obtained by varying 3-APTMS concentration and keeping cyclohexanone at constant concentration were examined by TEM images as given in Fig. 4.4- Fig. 4.7.

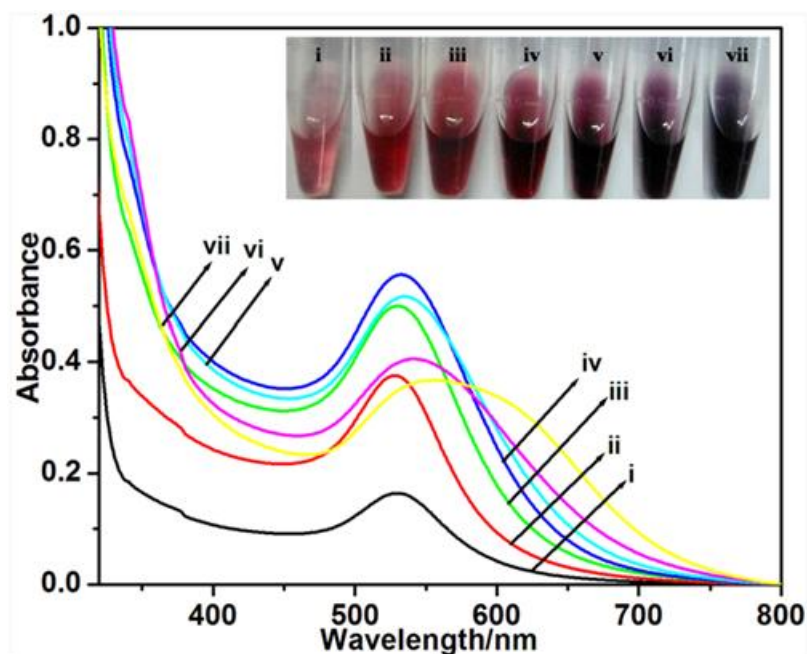


Figure 4.2. UV-Vis spectra showing change in  $\lambda_{\max}$  of AuNPs made using a constant concentration of cyclohexanone (4.8 M) and varying concentration of 3-APTMS (i) 3 mM (ii) 4 mM (iii) 6 mM (iv) 8 mM (v) 9mM (vi) 10 mM (vii) 12 mM.

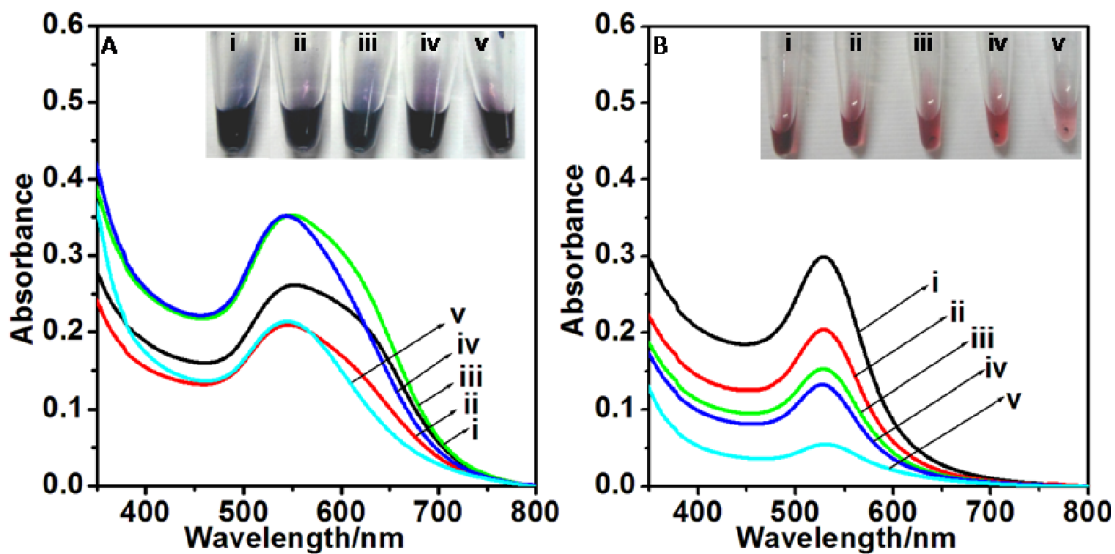


Figure 4.3. UV-Vis spectra showing change in  $\lambda_{\max}$  of AuNPs made using (A) constant concentration of 3-APTMS (10 mM) and varying cyclohexanone concentration (i) 1.0 M, (ii) 1.5 M, (iii) 2.0 M, (iv) 3.0 M (v) 4.0 M; (B) constant concentration of 3-APTMS (5 mM) and varying cyclohexanone concentration; (i) 4.0 M (ii) 5.0 M (iii) 6.0 M (iv) 7.0 M (v) 8.0 M.

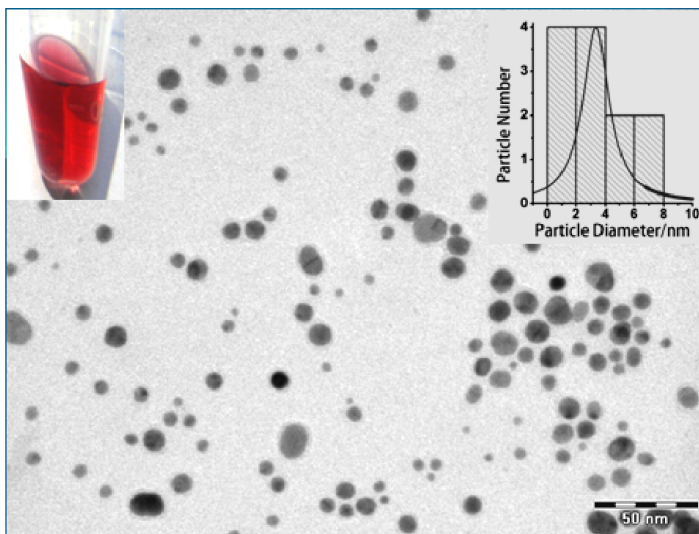


Figure 4.4. TEM images of AuNPs made using cyclohexanone (4.8 M) and 3-APTMS (8mM).

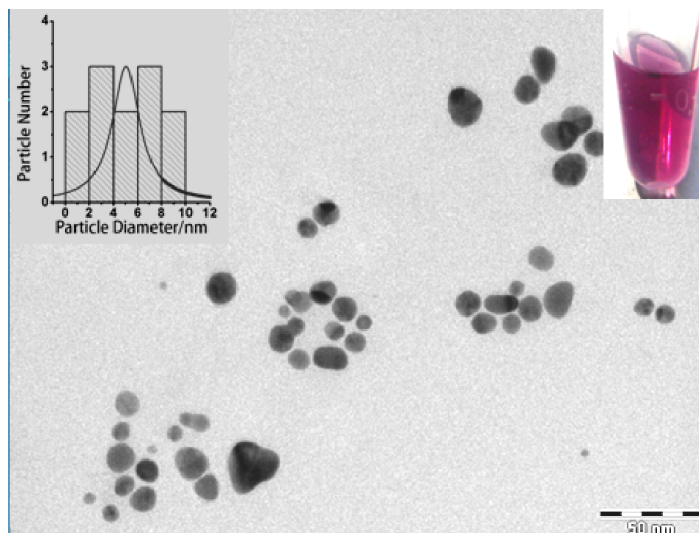


Figure 4.5. TEM images of AuNPs made using cyclohexanone (4.8 M) and 3-APTMS (10mM).

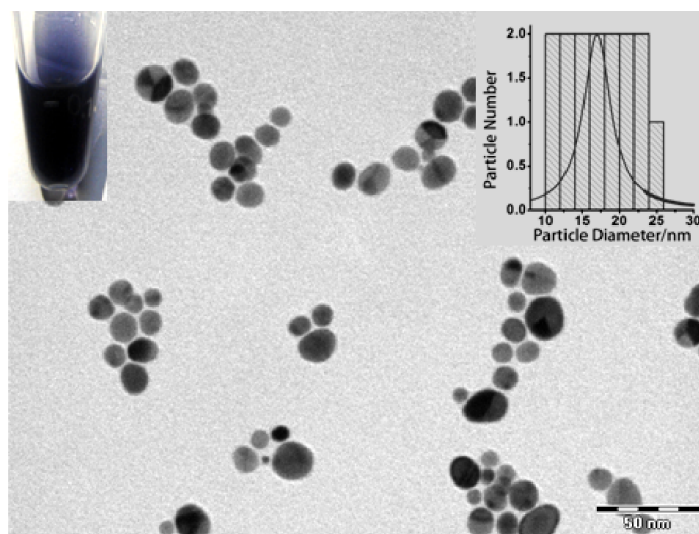


Figure 4.6. TEM images of AuNPs made using cyclohexanone (4.8 M) and 3-APTMS (12mM).

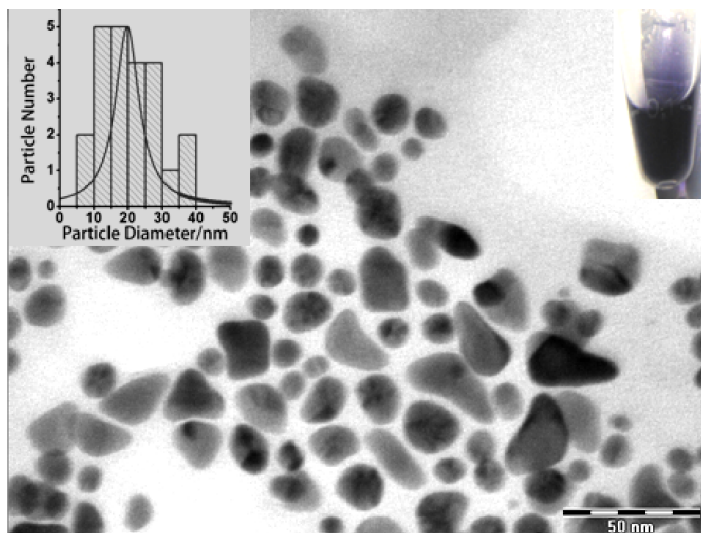


Figure 4.7. TEM images of AuNPs made using cyclohexanone (4.8 M) and 3-APTMS (15mM).

---

#### 4.3.3. Dispersibility of AuNPs made using 3-APTMS and acetone

In order to use as synthesized AuNPs for wider applications it has to be dispersible in most of the solvents. The solvents chosen in order to assess the compatibility of AuNPs, made using 3-APTMS and cyclohexanone are water, methanol and dichloromethane (DCM). Based on absorption spectra and visual photographs the dispersibility of AuNPs in above mentioned solvents has been monitored. AuNPs are profusely dispersible in DCM and methanol at all concentrations of 3-APTMS and cyclohexanone. However, the dispersibility of the same in water is affected at higher concentrations of cyclohexanone. Dispersibility of AuNPs made using different concentration of reactants (3-APTMS and cyclohexanone) in different solvents is shown in Fig. 4.8-Fig. 4.10. The dispersibility of AuNPs made using constant concentration of cyclohexanone and varying 3-APTMS concentration, in different solvents is shown in Fig. 4.8 and Fig.4.9.

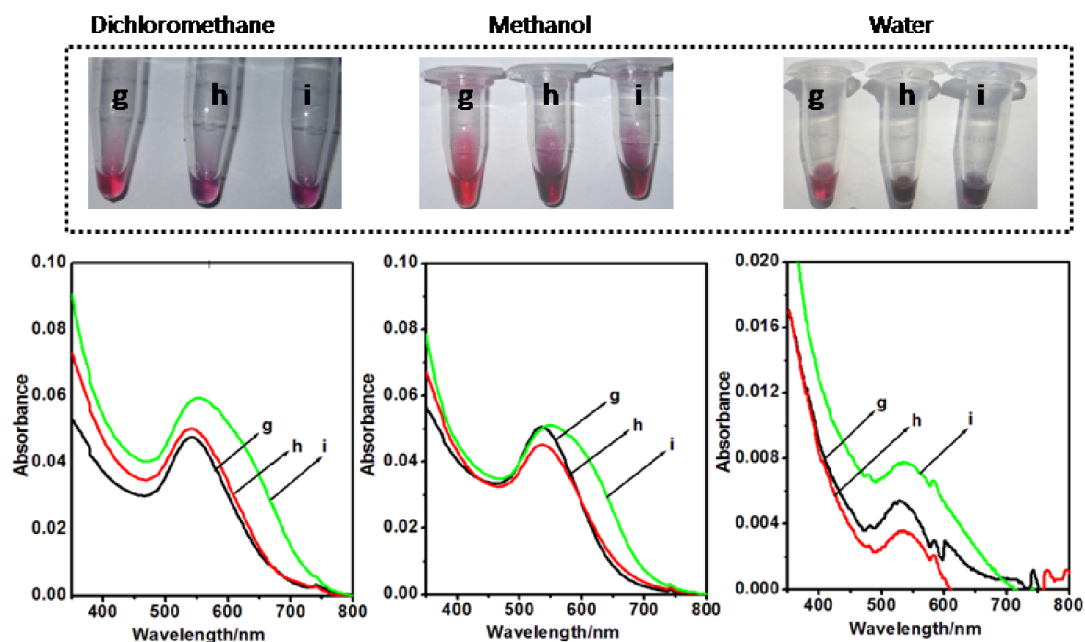


Figure 4.8. UV-Vis spectra of AuNPs and their dispersibility in DCM, methanol and water, made using constant concentration of cyclohexanone (4.8 M) and varying concentrations of 3-APTMS: (g) 5mM, (h) 7 mM, and (i) 9 mM. Images of corresponding AuNPs sol in the same solvents are shown as an inset to the image.

Similarly, Fig. 4.10 gives the dispersibility of AuNPs made using constant 3-APTMS concentration and varying cyclohexanone concentration in different solvents. The results indicate the problematic dispersion of AuNPs in water with increased cyclohexanone content. In order to make a detailed investigation on the dispersibility of AuNPs in organic solvents, the absorption spectra of the same as a function of AuNPs concentrations in water, DCM, acetonitrile and ethyl acetate are recorded, as shown in Fig. 4.11 and Fig. 4.12. The results show a linear relationship between the absorbance and the concentration of AuNPs with significant variation in  $\lambda_{\max}$  as a function of the nature of the solvents. The dependence of  $\lambda_{\max}$  on the refractive index and polarity index of these solvents is shown in Fig. 4.13.

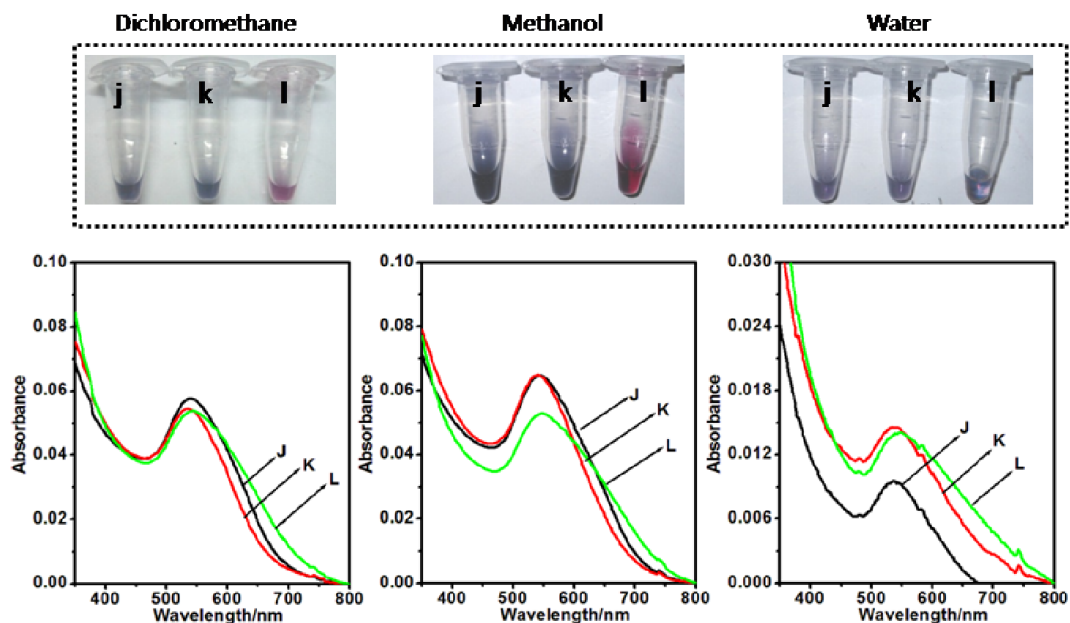
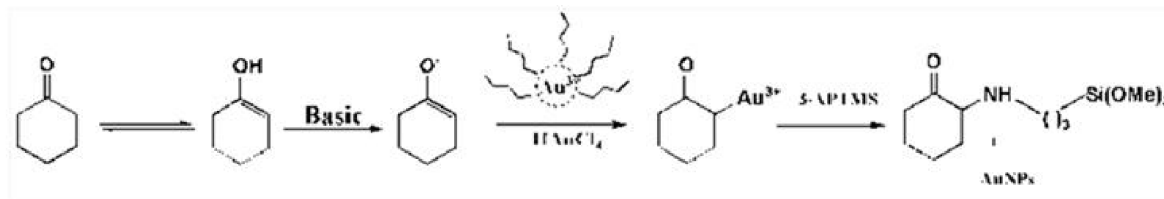


Figure 4.9. UV-Vis spectra of AuNPs and their dispersibility in DCM, methanol and water, made using constant concentration of cyclohexanone (3.8 M) and varying concentrations of 3-APTMS: (j) 5 mM, (k) 7 mM, and (l) 9 mM. Images of corresponding AuNPs sol in the same solvents are shown as an inset to the image.

#### 4.3.4. Catalytic ability of AuNPs

One of the important properties as proposed in Scheme 4.1 is the formation of an organic-inorganic hybrid between the organic amine linked to alkoxy silane and cyclohexanone. The formation of such a hybrid material enhances the catalytic properties of AuNPs compared to those in absence of the same.



Scheme 4.1. Proposed mechanism of 3-APTMS and cyclohexanone mediated synthesis of AuNPs.

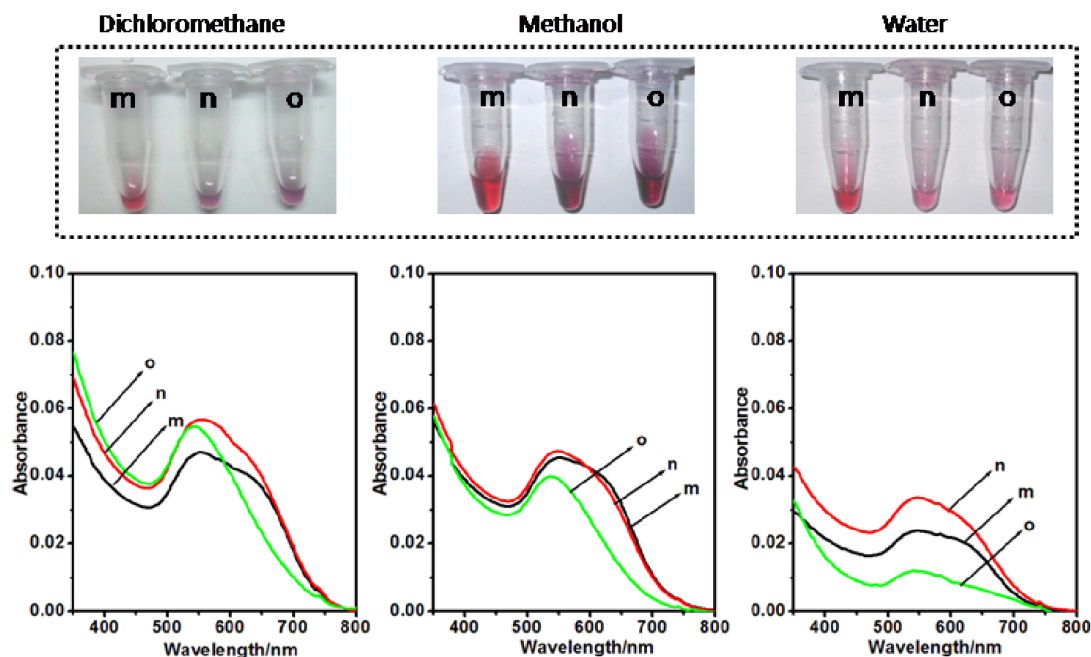


Figure 4.10. UV-Vis spectra of AuNPs and their dispersibility in DCM, methanol and water, made using constant concentration of 3-APTMS (10 mM) and varying concentrations of cyclohexanone: (m) 0.9 M, (n) 1.8 M, and (o) 3.8 M. Images of corresponding AuNPs sol in the same solvents are shown as an inset to the image.

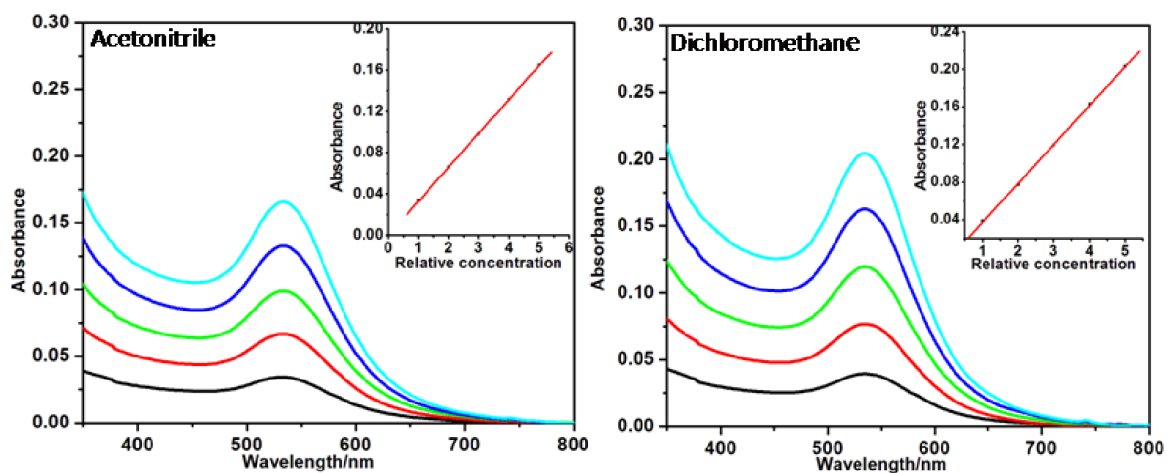


Figure 4.11. UV-Vis spectra of AuNPs in (i) acetonitrile (ii) dichloromethane. Inset shows the dependence of absorption maxima ( $\lambda_{\max}$ ) on relative concentration.

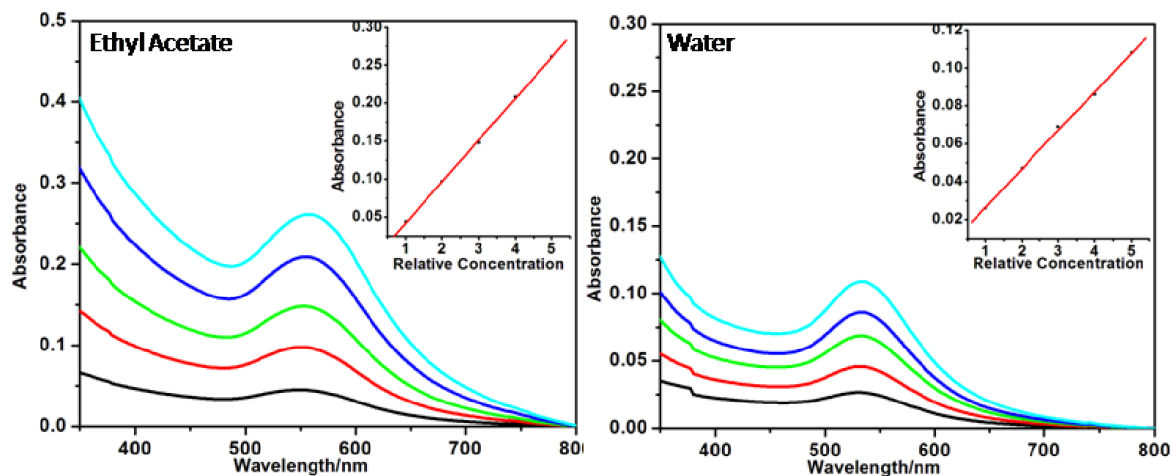


Figure 4.12. UV-Vis spectra of AuNPs in (i) Ethyl acetate (ii) water. Inset shows the dependence of absorption maxima ( $\lambda_{\max}$ ) on relative concentration.

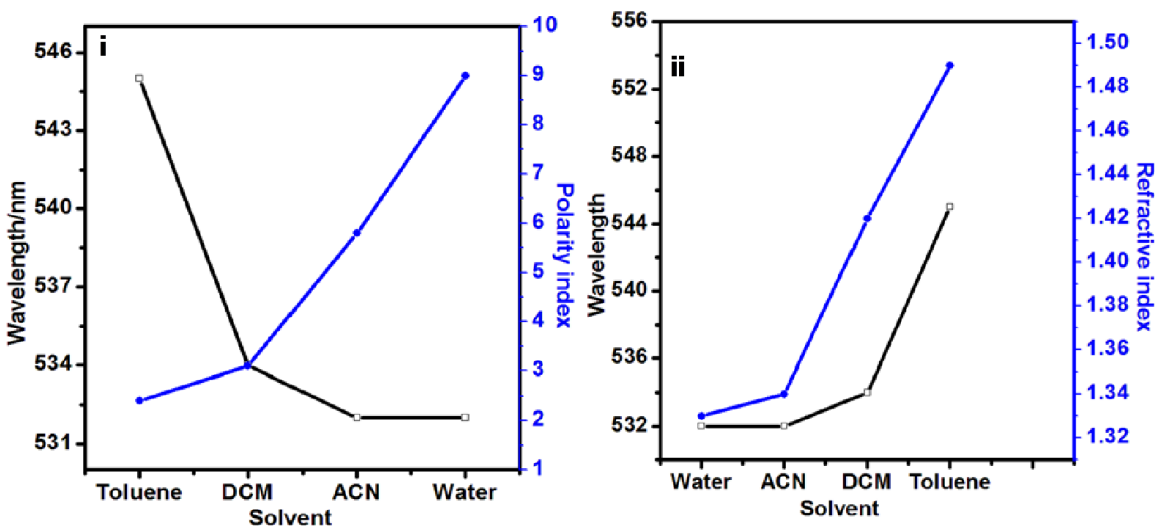


Figure 4.13. Dependence of  $\lambda_{\max}$  on polarity index (i) and refractive index (ii).

Therefore, an increase in 3-APTMS concentration will allow an increase in catalytic activity. Cyclohexanone mediated AuNPs synthesized at different 3-APTMS concentrations were checked for their catalytic behavior as peroxidase mimetics that allow the catalytic oxidation of o-dianisidine in the presence of  $H_2O_2$  as shown below



The catalytic behaviour of AuNPs can be examined from the absorption maxima of the oxidized product of o-dianisidine close to 430 nm. Catalytic behavior of AuNPs is found to increase with increasing 3-APTMS concentration irrespective of their size, as shown in Fig. 4.14. (A)–(D).

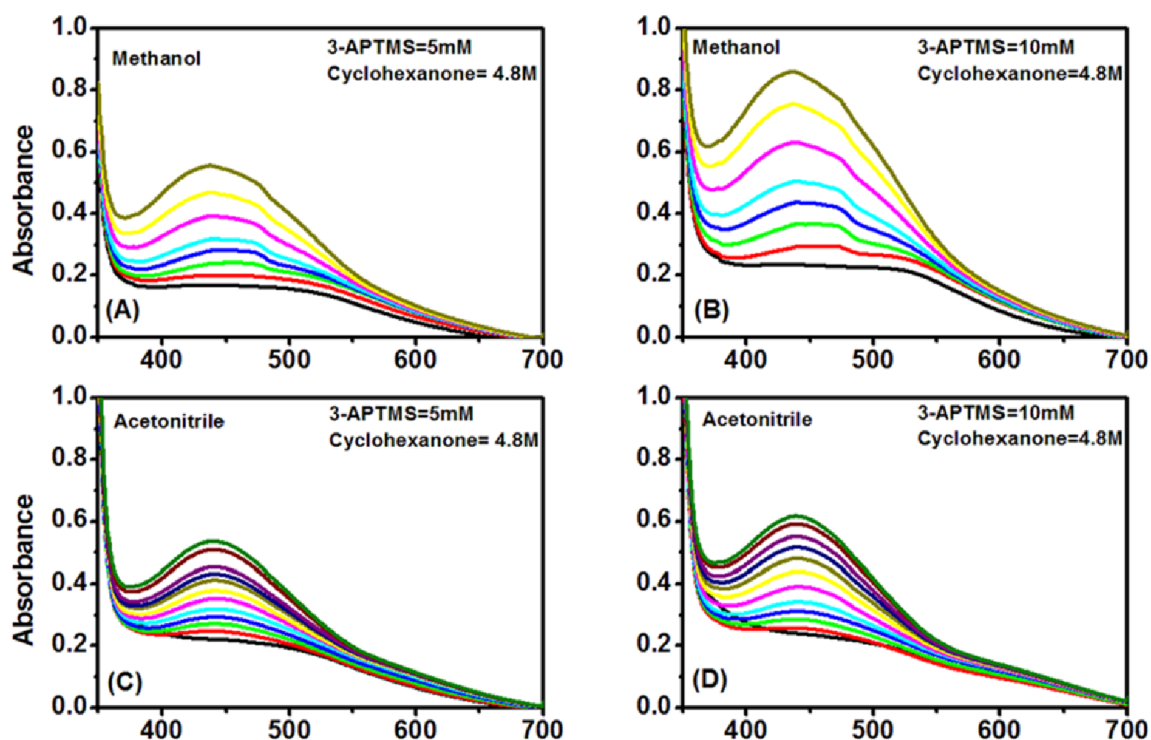
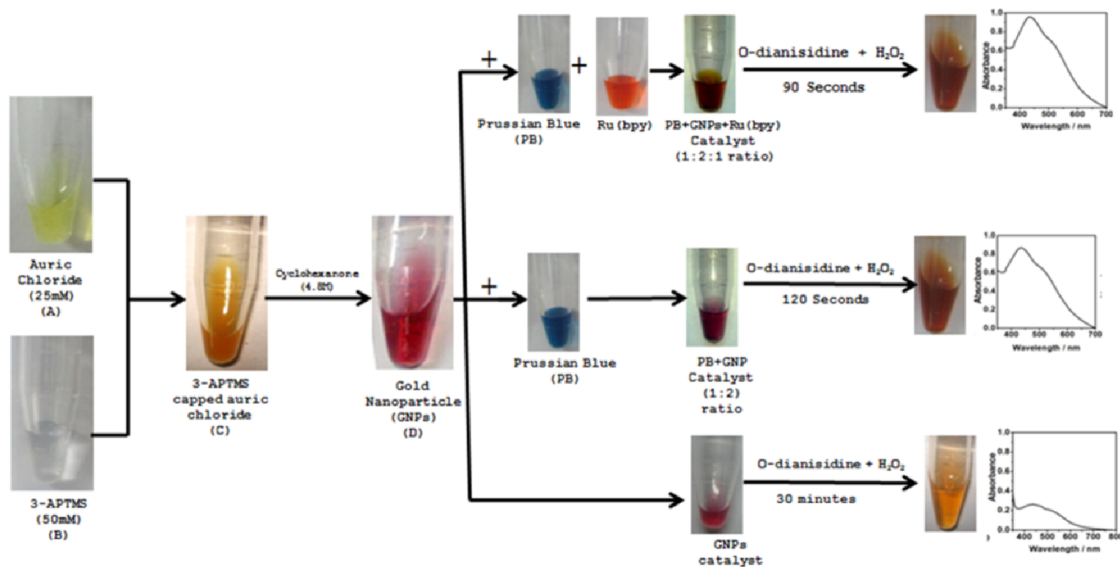


Figure 4.14. UV-Vis spectra of o-dianisidine–H<sub>2</sub>O<sub>2</sub> system catalyzed by AuNPs, fabricated using different 3-APTMS concentration, in methanol (A and B) acetonitrile (C and D), justifying the role of functional ability.

The AuNPs are not very good peroxidase mimic but their composite with Prussian blue improves the catalytic behavior. The possibility of nanocomposite formation is favored more because the reacting systems of both PBNPs and AuNPs possess similar reaction products, resulting in the formation of monophasic dispersions useful for homogenous

catalysis. Further, the use of Tris (2, 2-bipyridyl) ruthenium [Ru(bpy)] has been sought to enhance the performance of the nanocomposite. Ru(bpy) is an important optical material, which displays capping affinity with 3-APTMS and retains inherent photoactivity [Qian and Yang, (2007); Gill and Thomas, (2012)]. This property of Ru(bpy) prompted its use for the formation of a nanodispersion with the 3-APTMS functionalized nanocomposite of PBNPs and AuNPs, and indeed the excellent monophasic nanomaterial for homogenous catalysis was obtained. The schematic representation of peroxidase mimetic activity is shown in Scheme 4.2, depicting the ratio of various components participating in the formation of the nanocomposite dispersion. It is to be noted from the details given in Scheme 4.2 that when 3-APTMS (B) is added in methanolic gold salt solution (A), a dark yellow coloured product (C) is formed, justifying the specific interaction of gold ions with 3-APTMS. The formation of the nanocomposite dispersion of as synthesized AuNPs was examined by mixing each component under ambient conditions. Fig. 4.15 shows the UV-Vis spectra of AuNPs, PBNPs, PBNPs–AuNPs and PBNPs–AuNPs–Ru(bpy). The peroxidase mimetic ability of the AuNPs, AuNPs–PBNPs and the AuNPs–PBNPs–Ru(bpy) nanocomposite has been examined shown in Fig. 4.16 (i)–(iii) respectively for the o-dianisidine–H<sub>2</sub>O<sub>2</sub> system. The K<sub>m</sub> value for AuNPs, AuNPs–PBNPs and AuNPs–PBNPs–Ru(bpy) was calculated from the results shown in Fig. 4.17. Similarly by measuring the amount of H<sub>2</sub>O<sub>2</sub> produced using AuNPs–PBNPs–Ru (bpy)-o-dianisidine system from glucose-Gox system the glucose concentration can also be calculated. A typical glucose concentration–response curve is shown in Fig. 4.18 and the inset shows the corresponding calibration plot. The findings on peroxidase mimetic activity have been recorded using o-dianisidine as a substrate that shows maximum absorption at 430 nm.



Scheme 4.2. Schematic representation of various stages of nanocomposite formation for homogeneous catalysis.

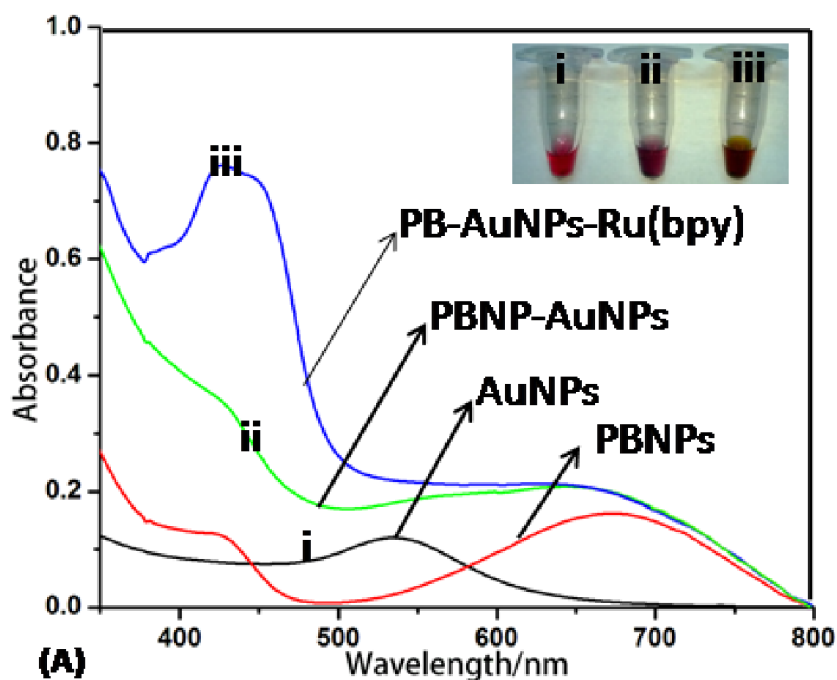


Figure 4.15. UV-Vis spectra of AuNPs (i), PBNPs–AuNPs (ii), PBNPs–AuNPs–Ru(bpy) (iii). Inset shows the visual images of the same.

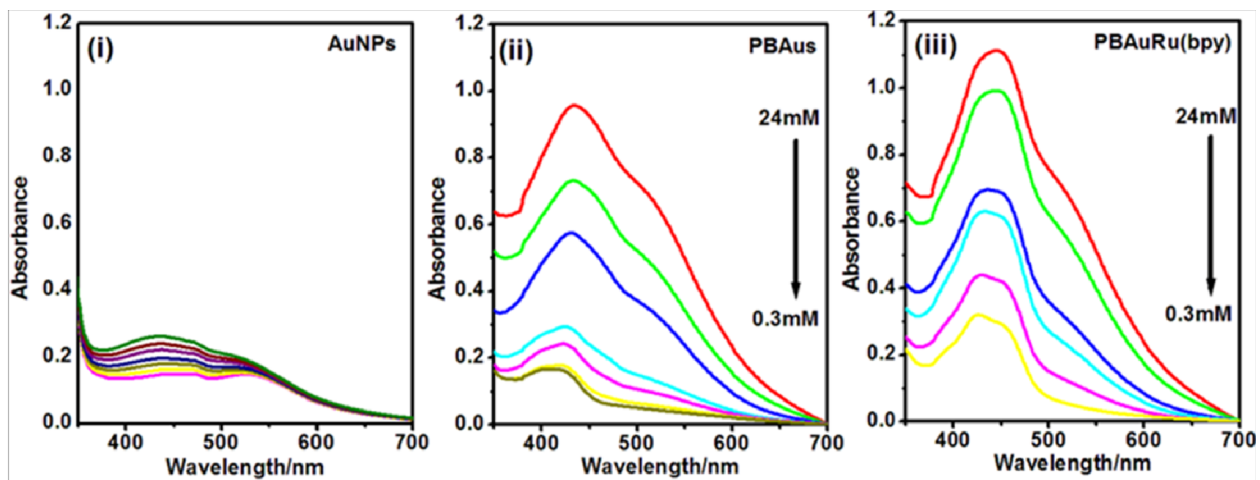


Figure 4.16. UV-Vis spectra of the *o*-dianisidine–H<sub>2</sub>O<sub>2</sub> system catalyzed by AuNPs (i), PBNP–AuNPs (ii), and PBNP–AuNPs–Ru(bpy) (iii).

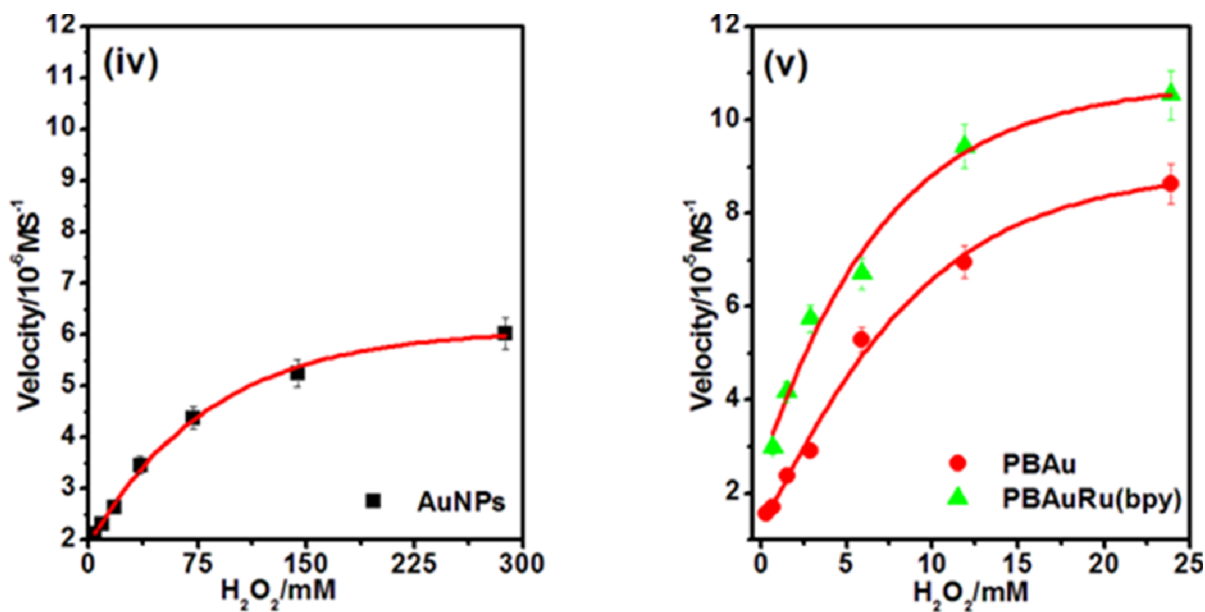


Figure 4.17. Kinetic analysis of *o*-dianisidine–H<sub>2</sub>O<sub>2</sub> system catalyzed by AuNPs (iv), PBNPs–AuNPs and PBNPs–AuNPs–Ru(bpy) (v).

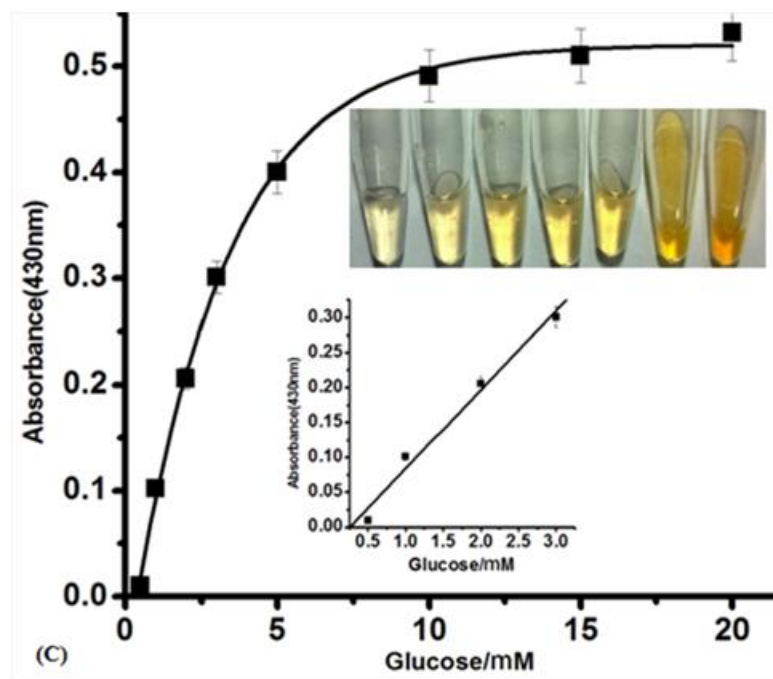


Figure 4.18. Response curve for glucose detection using glucose oxidase catalyzed formation of  $H_2O_2$  monitored by PBNP–AuNP–Ru(bpy)–o-dianisidine system; inset to [C] shows linear calibration plot for glucose and images show colour change as a function of glucose concentrations.

#### 4.3.5. Electrocatalytic ability of AuNPs and their nanocomposite

The results of the peroxidase mimetic ability of AuNPs based on UV-Vis spectroscopy directed us to evaluate their electrocatalytic ability for wider practical application of the nanomaterial. Since AuNPs are not the potential electroactive species required for the precise evaluation of electrocatalytic performance, it was convenient to make a nanocomposite with known potential redox material for such an investigation and the choice of Prussian blue (PB) again seemed to be reasonable. Because the evaluation of electrocatalytic ability for practical application is based on the dynamics of oxidation and

reduction of PB–AuNPs and subsequent measurement of electron exchange during electrochemical sensing, the role of 3-APTMS present in the nanocomposite could play a crucial role as 3-APTMS serves as a potential electron donor in polar media (Scheme 4.1) during AuNPs synthesis. The results shown in Fig. 4.17 depicted the application of PBNPs made from 3-APTMS and cyclohexanone as reported earlier (Pandey and Pandey, 2013). A similar nanocomposite for electroanalytical application may introduce severe problems during efficient electron transfer due to the large concentrations of 3-APTMS and may require detailed investigation. Accordingly, PB made using conventional protocol (potassium hexacyanoferrate and ferrous sulphate) was chosen to make a nanocomposite with gold nanoparticles of two different sizes AuNP1 (blue) and AuNP2 (red) in order of increasing nanogeometry. The as prepared PB–AuNPs were adsorbed on graphite particles and incorporated into a graphite paste electrode for understanding heterogeneous electrocatalysis based on probing the electrochemical behavior of a surface concerned redox species. Fig. 4.19(a)–(c) shows the voltammograms of these modified electrodes for PB (a), PB–AuNP1(b) and PB–AuNP2(c) at different scan rates in 0.1 M phosphate buffer (pH 7.0) containing 0.5 M KCl. Fig.4.20 gives the plot for anodic and cathodic peak current density vs scan rate and square root of scan rate. Because PB is used as an artificial peroxidase, the finding of the electrocatalytic reduction of  $\text{H}_2\text{O}_2$  at the surface of the modified electrodes has also been investigated. Fig. 4.21(a)–(c) shows the voltammograms of these modified electrodes in the absence (1) and the presence (2) of 2 mM  $\text{H}_2\text{O}_2$  in 0.1 M phosphate buffer, pH 7.0 at the scan rate of  $10 \text{ mVs}^{-1}$  for PB (a), PB–AuNP1(b) and PB–AuNP2(c). Finally, amperometric analysis of  $\text{H}_2\text{O}_2$  was done at constant operating potential of 0.05 V vs., Ag/AgCl in 0.1 M phosphate buffer pH 7.0 as shown in Fig. 4.22 for PB (a), PB–AuNP1 (b) and PB–AuNP2 (c).

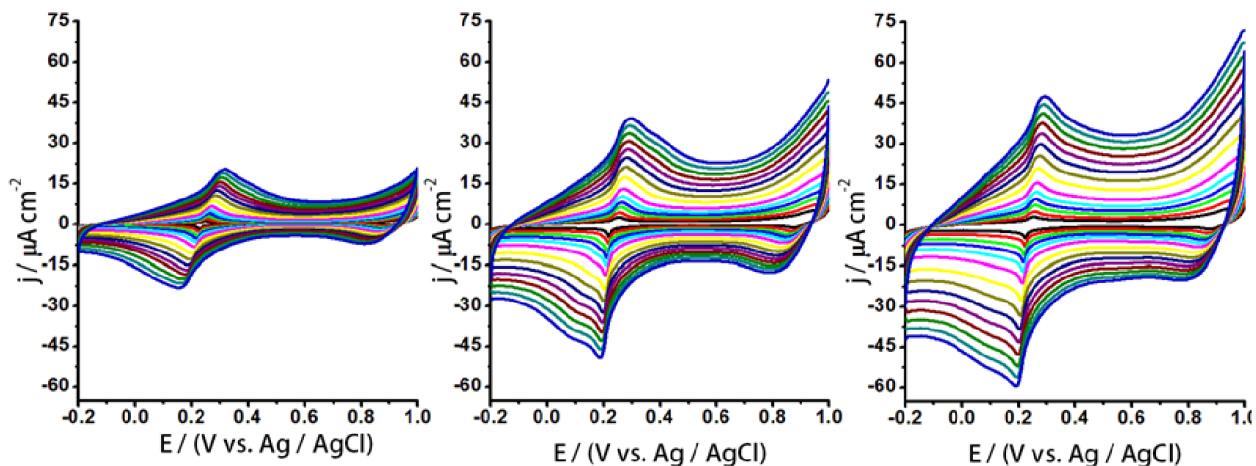


Figure 4.19. Cyclic voltammograms of PB (a), PB-AuNP1 (b) and PB-AuNP2 (c) in 0.1 M phosphate buffer of pH 7.0, containing 0.5 M KCl at the scan rates of 0.01, 0.02, 0.035, 0.050, 0.070, 0.10, 0.15, 0.20, 0.25, 0.30, 0.35, 0.40, 0.45, 0.50  $\text{V s}^{-1}$ .

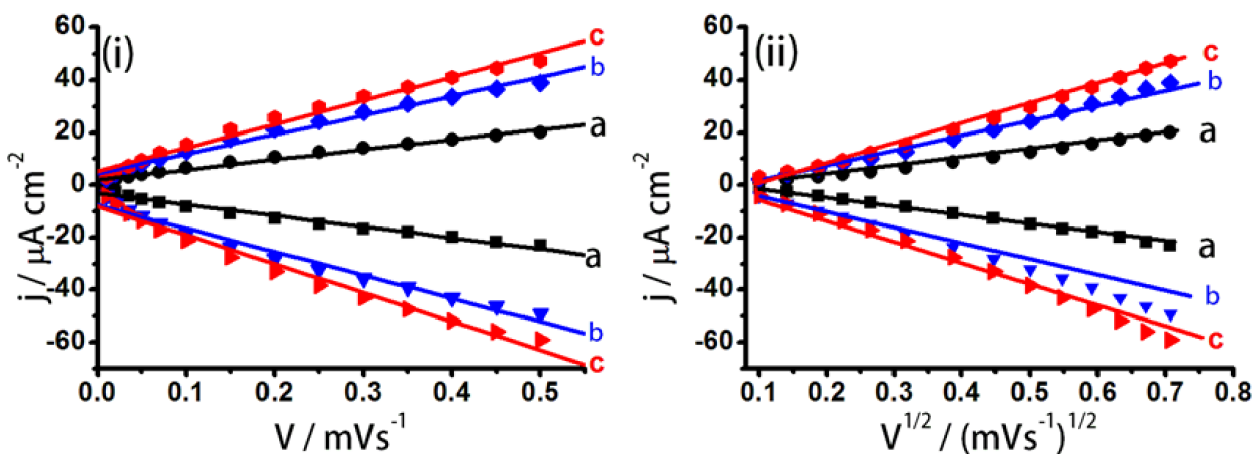


Figure 4.20. Show the plot of anodic and cathodic current density vs scan rate (i) and square root of scan rate (ii) respectively

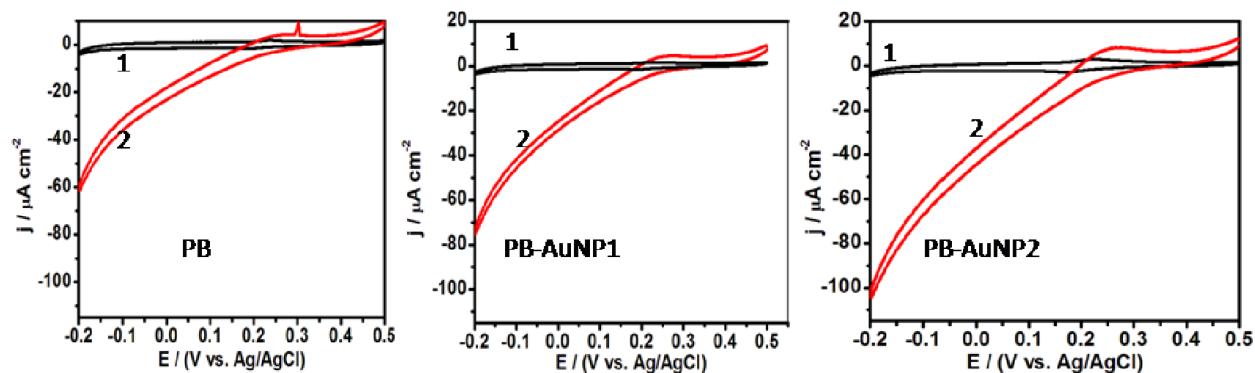


Figure 4.21. Cyclic voltammograms of PB, PB–AuNP1 and PB–AuNP2 in absence (1) and the presence (2) of 2 mM  $\text{H}_2\text{O}_2$  in 0.1 M phosphate buffer of pH 7.0 containing 0.5 M KCl at the scan rate of  $0.01 \text{ V s}^{-1}$ .

#### 4.4. DISCUSSION

The synthesis of AuNPs from the action of THF-HPO or cyclohexanone over 3-APTMS capped  $\text{Au}^{3+}$  has been monitored spectrophotometrically as a function of time as shown in Fig. 4.1. The figure clearly shows the appearance of peak at  $\sim 520\text{nm}$ , corresponding to AuNPs, with gradual increase in its absorbance value as a function of time.

##### 4.4.1. Cyclohexanone and 3-APTMS role during AuNPs synthesis

Further the effect of the increasing concentration of 3-APTMS and cyclohexanone on the  $\lambda_{\text{max}}$  value of the AuNPs has been monitored as given in Fig. 4.2 and Fig. 4.3, and it was found that  $\lambda_{\text{max}}$  value showed red shift with increasing 3-APTMS concentration and blue shift with increasing cyclohexanone concentration which gives an idea about the change in size of AuNPs. There is a well established relationship between AuNPs size and plasmon band position, with the plasmon resonance band shifting to the red and broadening with increasing particle size (Aslam et al., 2004).

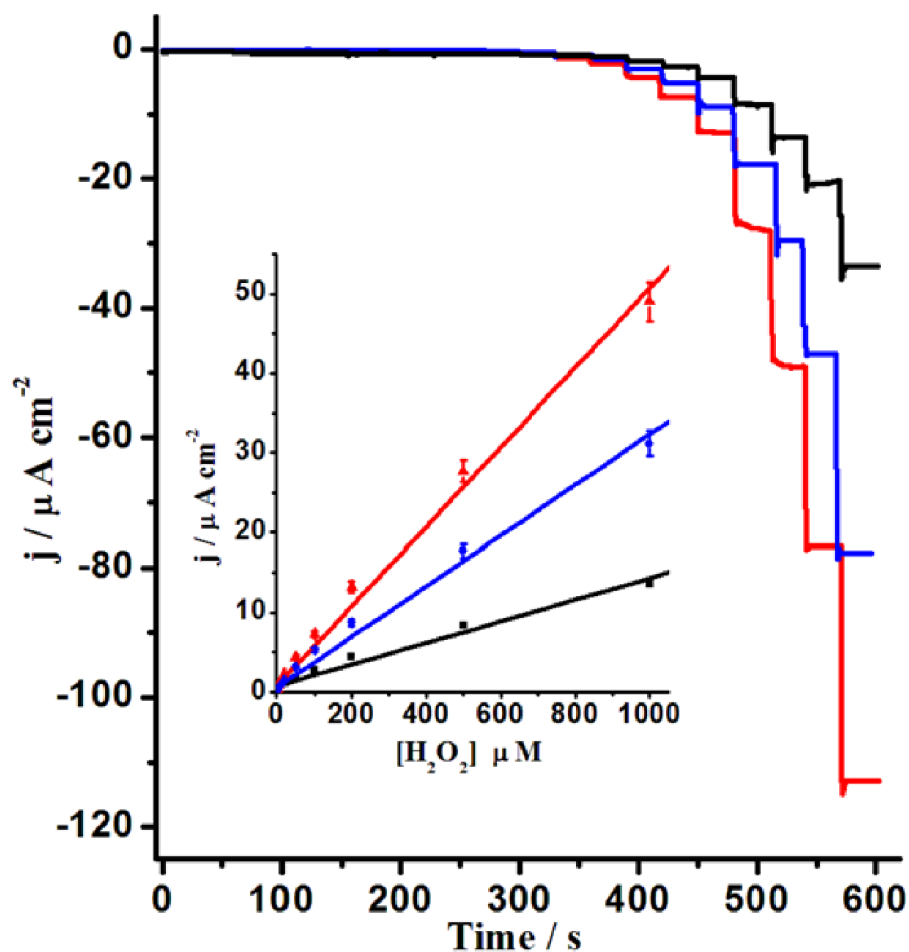


Figure 4.22. Amperometric response of  $\text{H}_2\text{O}_2$  analysis at 0.05 V vs. Ag/AgCl in 0.1 M phosphate buffer of pH 7.0, containing 0.5 M KCl, inset to [3] shows the linear range of calibration curves for PB (a), PB-AuNP1(b) and PB-AuNP2(c).

These findings based on UV-Vis spectroscopy show that there is a maximum and minimum limit of 3-APTMS (3–15 mM) and cyclohexanone (1.0–7.0 M) concentrations, beyond which the synthesis of AuNPs does not occur. Such specific requirements of 3-APTMS and cyclohexanone could be possible due to micellar characteristics and the requirement of critical micellar concentration (CMC) of the analytes. Below 3 mM and above 15 mM there was no sign of AuNPs formation at any cyclohexanone concentration. Such limitation may also be linked to specific CMC of cyclohexanone during 3-APTMS mediated

conversion of nanoparticles. An optimum concentration of each component is required for AuNPs due to micellar behavior of 3-APTMS. TEM images of AuNPs corresponding to increasing concentration of 3-APTMS have been given in Fig. 4.4- Fig.4.7 revealing the range of average size of 3–45 nm corresponding to 3-APTMS concentrations of 8 mM, 10 mM, 12 mM and 15 mM at 4.8 M cyclohexanone.

#### **4.4.2. Proposed mechanism for interaction between 3-APTMS and cyclohexanone during AuNPs synthesis**

The proposed mechanism for the 3-APTMS and cyclohexanone mediated synthesis is shown in Scheme 4.1. Cyclohexanone in the prevailing medium undergoes keto–enol tautomerism. The enolate ion acts as an electron donor to the 3-APTMS capped  $\text{Au}^{3+}$  ion, which in turn acts as a Lewis acid, leading to the formation of AuNPs. It is important to compare the role of other reducing agents like 3-GPTMS and THF-HPO with cyclohexanone required for the synthesis of AuNPs. Organic moieties (3-GPTMS, THF-HPO and cyclohexanone) used for the synthesis of 3-APTMS and  $\text{Au}^{3+}$  mediated AuNPs differ in the following respects: (i) 3-GPTMS and cyclohexanone have an affinity for organic medium, whereas THF-HPO have affinity for aqueous medium, (ii) 3-GPTMS is a bulky group, whereas cyclohexanone and THF-HPO are comparatively smaller moieties, (iii) tendency of the reducing agents to form organic–inorganic hybrids during AuNPs synthesis and (iv) 3-GPTMS, THF-HPO and cyclohexanone have different CMC, allowing variable interaction with 3-APTMS capped gold ions during nanoparticle synthesis. The difference in properties of as synthesized AuNPs using different reducing agents is born out of these differences in their nature.

#### 4.4.3. Effect of organic reducing agents on the dispersibility of AuNPs

Dispersibility of AuNPs largely depends on the medium, which in turn is determined by the apparent polar or nonpolar behaviour of the organic moieties (3-GPTMS/THF-HPO/cyclohexanone) given that 3-APTMS is amphiphilic in nature. The results based on dispersibility of cyclohexanone and 3-APTMS mediated AuNPs in three different solvents viz. water, methanol and dichloromethane justified the use of AuNPs both in aqueous and non-aqueous media, however, increased concentration of cyclohexanone caused problem with its dispersibility in water as shown in Fig.4.8- Fig.4.10. The comparison on the dispersibility of this AuNPs have been made with the other AuNPs made using 3-GPTMS (chapter II) and THF-HPO (chapter III) in combination with 3-APTMS. The use of THF-HPO as mild reducing agent for the fabrication of 3-APTMS mediated AuNPs enables the dispersibility of AuNPs in aqueous and methanolic media, however, solvents like DCM and toluene reject the nanoparticle completely, resulting in a two phasic mixture as presented in Fig. 4.23. Dispersibility of AuNPs with 3-GPTMS as the organic reducing moiety in different media has been reported in second chapter where the nanoparticles were mostly dispersible in the organic phase with limited dispersibility in water. Thus it is concluded that the dispersibility of 3-APTMS capped AuNPs depends on the organic reducing agent (3-GPTMS, THF-HPO or cyclohexanone) used. Further to observe the compatibility of 3-APTMS and cyclohexanone mediated AuNPs with different solvents, relationship between absorbance and concentration of AuNPs in different solvents has been observed and found to vary linearly as shown in Fig. 4.11 and Fig. 4.12. Fig. 4.13 also shows the compatibility of AuNPs in different solvents in terms of polarity index and refractive index.

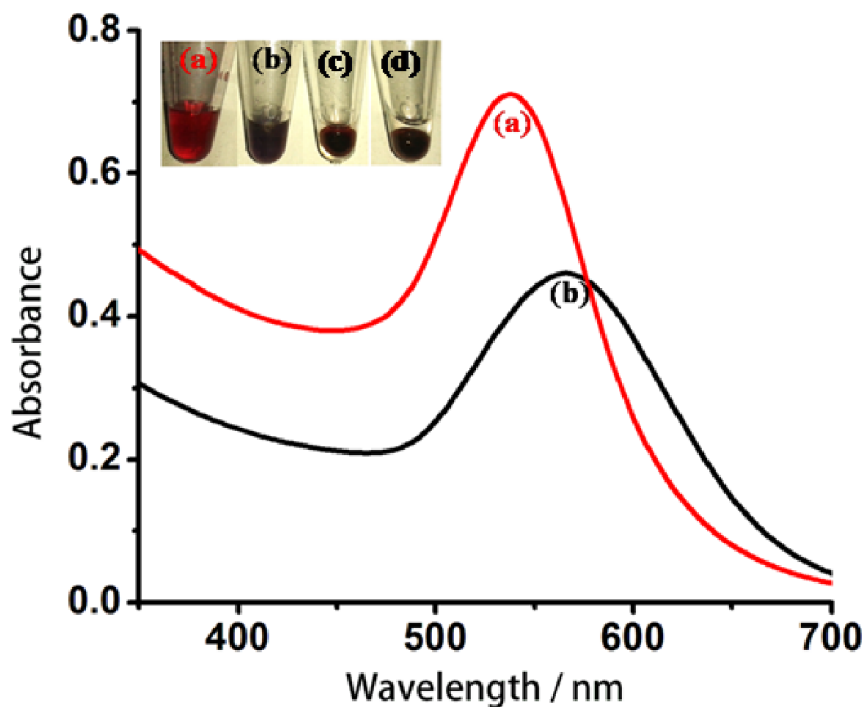


Figure 4.23. Dispersibility of AuNPs made using 3-APTMS and THF-HPO in water (a) methanol (b) dichloromethane and toluene (d).

---

#### 4.4.4. Effect of organic reducing agents on the catalytic ability of AuNPs

The results obtained from the Fig. 4.14 indicate that the the catalytic behaviour of AuNPs primarily depends on the functional ability of 3-APTMS rather than nanogeometry. Similar properties of AuNPs made from the use of THF-HPO have been observed in the last chapter. 3-GPTMS does not result in the formation of an organic-inorganic hybrid, thus catalysis largely depends on nanogeometry irrespective of 3-APTMS concentration. Investigating the use of AuNPs as a peroxidase mimetic resulted in a very high  $K_m$  value, which means it is too weak to be used as a peroxidase mimetic (Fig. 4.17). For a material to work as a potential substitute of peroxidase enzyme, it should be stable enough at room temperature and its peroxidase mimetic ability should be equivalent to, or higher than that

of the peroxidase enzyme under feasible experimental conditions. In addition to that, the resulting nanocomposite should have homogeneous dispersion in the reaction medium as per the requirements for homogeneous catalysis. Such requirements restrict the practical usability of many such catalytic materials due to poor solubility in the working solvent. Accordingly, there is need to improve the mimetic ability of AuNPs by making nanocomposites of the same having dispersibility for homogeneous catalysis. 3-APTMS and cyclohexanone mediated Prussian blue nanoparticles (PBNPs), behave as artificial peroxidases, the nanocomposite with as-synthesized AuNPs may be a perfect peroxidase replacement because the resulting PBNP–AuNPs nanocomposite is dispersible in aqueous medium. The addition of ruthenium bipyridyl Ru(bpy) to the PBNP–AuNPs nanocomposite as discussed in result section further enhances the peroxidase mimetic ability. The absorbance spectra for AuNPs, PBNPs, PBNP–AuNPs and PBNPs–AuNPs–Ru(bpy) show their characteristic peaks as given in Fig.4.15. The results demonstrate the formation of a nanocomposite dispersion for practical applications. The  $K_m$  value for AuNPs as calculated from Fig. 4.17 is found to be 30.4 mM, which means it is too weak to be used as a peroxidase mimic and the  $K_m$  for PBNPs–AuNPs comes out to be 4.6 mM, which is comparable to that recorded on using HRP under practical experimental conditions (Gao et al., 2007). Addition of Ru(bpy) to the nanocomposite further enhances the mimetic ability with a  $K_m$  value of 2.9 mM. The mimetic ability of the nanocomposite has been very effective in the precise probing of the glucose oxidase catalysed reaction. Based on the peroxidase like property of PBNP–AuNPs–Ru(bpy), the detection of glucose content was made by utilizing o-dianisidine as a chromogenic substrate analogous to that reported earlier based on the measurement of  $H_2O_2$  as a function of a GOx catalyzed reaction (Chen et al., 2012; Wei and Wang, 2008; Guascito et al., 2011). The  $H_2O_2$  formed

as a function of the GOx catalyzed oxidation of glucose was monitored spectrophotometrically using the oxidation product of o-dianisidine to indirectly measure the concentration of glucose as shown in Fig. 4.18. The linear range and lowest detection limit for glucose were found to be 0.5–3mM and 0.5 mM, respectively.

#### **4.4.5. Electrocatalysis of PB-AuNPs nanocomposite**

The nanocomposite of PB was made with two different sizes of AuNPs, made using two different concentrations of 3-APTMS, selected to see the effect of size and functionality on the electrocatalysis of redox species. Modified graphite paste electrode was made by mixing the nanocomposite with graphite paste. The results as seen in Fig. 4.19 (a)–(c) show the redox behavior of Prussian blue as a function of AuNPs nanogeometry and reveal faster electron exchange on increasing the nanogeometry of AuNPs as evaluated from the plots (i) and (ii) of Fig.4.20, for the respective voltammograms. The results as shown in Fig. 4.21 (a)–(c) clearly reveal subsequent enhancement in electrocatalytic property as a function of AuNPs nanogeometry. Linear range of calibration curves for PB (a), PB–AuNP1 (b) and PB–AuNP2 as shown in Fig.4.22 again confirm the role of AuNPs nanogeometry on electrocatalysis and justify an increase of the same on increasing nanogeometry

#### **4.4.6. Effect of organic reducing agents on the stability of AuNPs**

A comparative study on the stability of AuNPs made from the use of 3-APTMS capped gold ions in the presence of 3-GPTMS, THF–HPO and cyclohexanone has been made and it has been found that cyclohexanone as a reducing agent is most stable among three. Although 3-GPTMS mediated AuNPs remained stable as a suspension for a long time (>90 days), they suffered the problem of hydrolysis due to the Si–O–Si linkage, which was

reduced several fold when 3-GPTMS was replaced by cyclohexanone. THF–HPO system although requires less concentration of 3-APTMS compared to 3-GPTMS but is not very stable as colloidal suspension and thus is least stable of the three.

#### **4.5. CONCLUSION**

To summarize, a comparative study on the role of organic reducing agents (3-GPTMS, THF–HPO and cyclohexanone) during 3-APTMS mediated controlled synthesis of AuNPs is presented. 3-APTMS-mediated AuNPs made using different reducing agents differ from each other in properties such as dispersibility, catalysis, stability etc. thus making them available for use in various applications. In a bid to get 3-APTMS mediated AuNPs having better stability and dispersibility than with THF–HPO and 3-GPTMS, cyclohexanone has been used, which ensures the formation of an organic–inorganic hybrid and facilitates the peroxidase mimetic ability of AuNPs. AuNPs can be made dispersible in different solvents (organic or aqueous) by adjusting the constituents' (3-APTMS/cyclohexanone) ratio. Thus, the use of different reducing agents having compatibility with different solvents results in AuNPs with significant variation in properties from each other, presenting the option to select AuNPs for specific applications either in aqueous or organic media. These nanoparticles display functional ability to form monophasic nanocomposites for homogeneous catalysis with Prussian blue nanoparticles and ruthenium bipyridyl for specific application as peroxidase mimetics. In addition to that, the nanoparticles also enable the formation of nanocomposites with Prussian blue useful as heterogeneous redox catalysts displaying excellent electrochemical properties as a function of nanogeometry. Both mimetic and electrocatalytic ability could be explored for probing glucose oxidase catalyzed reactions, justifying the potential viability in biomedical applications.